

Coordinated thermal and optical observations of Trans-Neptunian object (20000) Varuna from Sierra Nevada

E. Lellouch¹, R. Moreno², J.L. Ortiz³, G. Paubert⁴, A. Doressoundiram¹, and N. Peixinho^{1,5}

¹ Observatoire de Paris, 5, place J. Janssen, F-92195 Meudon, France
e-mail: emmanuel.lellouch@obspm.fr

² I.R.A.M. 300, av. de la Piscine, F-38406 St-Martin d'Hères Cedex, France

³ Instituto de Astrofísica de Andalucía, CSIC, Camino Bajo de Hueter 24, E-18080 Granada, Spain

⁴ I.R.A.M. Avda. Divina Pastora 7, E-18012 Granada, Spain

⁵ Centro de Astronomia e Astrofísica da Universidade de Lisboa, PT-1349-018 Lisboa, Portugal

Received ;

Abstract. We report on coordinated thermal and optical measurements of trans-Neptunian object (20000) Varuna obtained in January-February 2002, respectively from the IRAM 30-m and IAA 1.5 m telescopes. The optical data show a lightcurve with a period of 3.176 ± 0.010 hr, a mean V magnitude of 20.37 ± 0.08 and a 0.42 ± 0.01 magnitude amplitude. They also tentatively indicate that the lightcurve is asymmetric and double-peaked. The thermal observations indicate a 1.12 ± 0.41 mJy flux, averaged over the object's rotation. Combining the two datasets, we infer that Varuna has a mean 1060^{+180}_{-220} km diameter and a mean $0.038^{+0.022}_{-0.010}$ V geometric albedo, in general agreement with an earlier determination using the same technique.

Key words. Kuiper belt – Planets and satellites: general – Techniques: photometric – Submillimeter

1. Introduction

Our view of the outer Solar System has changed dramatically over the last decade, with the discovery of hundreds of objects beyond Neptune's orbit. These trans-Neptunian objects (TNOs), which can be classified in three dynamical groups from their orbital properties, are believed to have formed in the tenuous outskirts of the protoplanetary disk, and to have remained relatively unaltered since then (e.g. Jewitt & Luu 2000). As such, and since they are also thought to be the source of short-period comets (Duncan et al. 1988), these bodies are currently the subject of considerable interest. Because of their intrinsic faintness, however, the physical and chemical properties of TNOs are difficult to study. For most of them, physical observations are restricted to broad-band photometry, providing magnitudes, colors, and rotation periods (e.g. Doressoundiram et al. 2001, 2002). Only for a few of them have infrared spectra been acquired, with compositional diagnostics.

Among this population, the “classical TNO” (20000)Varuna, discovered in November 2000 under the provisional designation of 2000 WR₁₀₆ (McMillan & Larsen 2000), has received special attention. Thanks to predisccovery observations dating back to 1955 (Knoffel & Stoss 2000), its orbit is accurately known (to within

0.1 arcsec). With an apparent visual magnitude of about 20.3 (absolute visual magnitude, $H=3.7$), it is one of the brightest known TNOs, being as of today surpassed only by (28978)Ixion ($H=3.2$). Visible photometry indicates that Varuna is moderately red ($B-R \sim 1.5$) (Jewitt & Sheppard 2002, hereafter JS02; Doressoundiram et al. 2002), and near-IR spectroscopy suggests the presence of water ice bands at 1.5 and 2.0 μm (Licandro, Oliva & Di Martino, 2001). Jewitt, Aussel & Evans (2001, hereafter JAE01) reported the detection of Varuna at 850 μm from JCMT observations, with a flux of 2.81 ± 0.85 mJy. From the combination of this thermal emission measurement with simultaneous optical observations, they inferred an equivalent circular diameter of 900^{+129}_{-145} km and a red geometric albedo of $p_r = 0.070^{+0.030}_{-0.017}$. Shortly after, Farnham (2001) reported that Varuna's exhibits a rotational lightcurve, with a 0.5 mag amplitude and a single-peaked period of 3.17 hour, although periods of 2.78 and 3.67 hours could not be ruled out. The rotational behaviour of Varuna was extensively investigated by JS02 who reported a two-peaked R lightcurve with period 6.3442 ± 0.0002 hour and 0.42 ± 0.02 mag amplitude, and no rotational variations in the visible colors (B-V, V-R, V-I). They concluded that Varuna is probably an elongated, prolate body with a (projected) axis ratio as high as 1.5:1.

We present here additional combined observations of Varuna in the thermal and visible range, performed from two telescopes (IRAM-30m and IAA 1.5m, respectively), located on Pico Veleta, Sierra Nevada (southern Spain). The prime goal was to obtain an independent measurement of Varuna's thermal flux to confirm the single detection of JAE01. A secondary, more difficult, objective was to search for rotational variability in the thermal flux. Indeed, a positive correlation of the thermal lightcurve with the optical lightcurve would indicate a shape effect (as is possibly the case for Ceres (Altenhoff et al. 1996) and Vesta (Redman et al. 1992)), while anticorrelation is the manifestation of albedo markings (an example is Pluto, Lellouch et al. 2000a). Unfortunately, our thermal observations did not prove of sufficient quality for this goal.

2. Observations

2.1. Optical observations

Optical observations were carried out at the 1.5m telescope of Sierra Nevada Observatory during a 1-week run in February 2002. Unfortunately, weather conditions allowed observations only in two of the nights (Feb. 8 and 9). The seeing varied from 1.0 arcsec to 1.7 arcsec, with an average of ~ 1.5 arcsec.

The 1.5m telescope was equipped with a fast readout 1024x1024 CCD camera based on a Kodak KAF1001E chip with square ~ 0.41 arcsec pixels and a 7×7 arcmin field of view. To maximize the signal-to-noise, we did not use any filter. The covered wavelength range is 350-940 μm , with maximum sensitivity at 580 nm. Integration times were typically 100 sec, and a S/N of ~ 15 was achieved for most of the images. More than 300 images were obtained and analyzed. Typical drift rates for Varuna (2.2 arcsec/hour in right ascension and 0.3 arcsec/hour in declination) were well below the seeing disc size in our 100-sec exposures. We used a fast readout CCD, whose read noise was still significantly lower than the typical shot noise from the sky background.

The reduction of the data was carried out following a standard processing including average bias subtraction and flatfield correction using high S/N twilight sky flatfields. The DAOPHOT package was used for the synthetic aperture calculations. Several synthetic apertures were tried for the objects and field stars. We adopted the aperture that gave the lowest scatter in the data. It corresponds to a diameter of 8 pixels. This is consistent with the conclusion of Barucci et al. (2000) that optimum photometry is achieved for an aperture a few pixels wider than the full width at half maximum of the star profiles in the worst seeing images. The fraction of flux loss in this relatively small 8-pixel diameter apertures was computed by measuring the percentage of flux loss on the brightest non-saturated stars in the images, and the final results were corrected for this aperture effect. From the dispersion of the data we estimate that the average

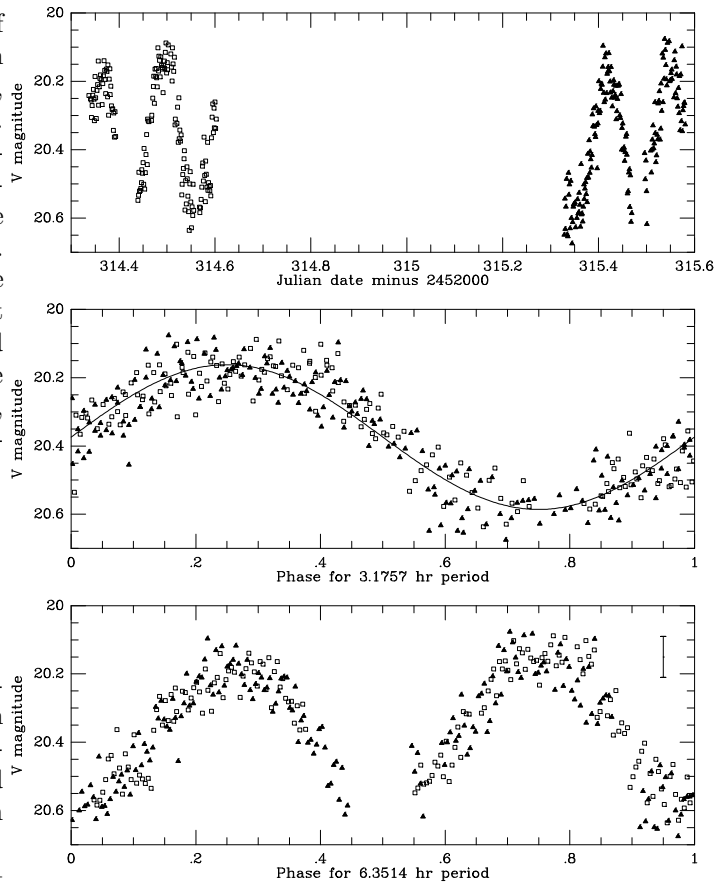


Fig. 1. Optical observations of Varuna. Top: V magnitude vs. (J-2452000) date. Middle: V magnitude vs. rotational phase, for a period of 3.1757 hr, and sinusoidal fit. Bottom: Same for a period of 6.3514 hr. A reference 0.25 phase is taken on Julian date 2452314.3591. Squares represent observations on the night of Feb. 8, 2002, and triangles correspond to observations on the night of Feb. 9, 2002. The error bar on the bottom graph indicates the ± 0.06 mag relative uncertainty of the individual photometric measurements.

error of the 100-sec exposures was 0.06 mag, close to theoretical expectations.

Photometry was performed relative to seven field stars, observed within the field of view. The same set of stars was used for the two observing nights. Since our broadband observations do not correspond to any of the photometric Johnson bands, the relative magnitudes were placed in an absolute scale using observations of Landolt standard stars (Landolt 1992) with colors similar to those of Varuna, in order to minimize any uncertainties in the flux calibration that could arise from color effects. The uncertainty in the absolute calibration due to a slight difference in colors is estimated to be ± 0.08 mag. This source of error dominates the uncertainty in the absolute photometry. All our photometric measurements are listed in Table 1.

A period search routine based on the Lomb (1976) technique was applied to the reduced data. A periodic signal of 3.1757 h was found, with a 0.42 ± 0.01 magnitude amplitude. The 0.01 mag uncertainty is the 1σ un-

Table 1. V-band photometry of Varuna

UT ^a	JD ^a	m _v	UT ^a	JD ^a	m _v
Feb. 02	2452300+		Feb. 02	2452300+	
8.8371	14.33712	20.241	8.9583	14.45828	20.444
8.8402	14.34020	20.251	8.9595	14.45948	20.310
8.8414	14.34139	20.254	8.9607	14.46069	20.316
8.8426	14.34259	20.306	8.9619	14.46190	20.318
8.8438	14.34381	20.271	8.9671	14.46709	20.315
8.8450	14.34500	20.241	8.9683	14.46830	20.299
8.8462	14.34622	20.224	8.9699	14.46995	20.249
8.8474	14.34743	20.252	8.9712	14.47116	20.215
8.8486	14.34863	20.315	8.9724	14.47236	20.185
8.8499	14.34985	20.185	8.9736	14.47356	20.264
8.8510	14.35105	20.248	8.9748	14.47478	20.164
8.8525	14.35253	20.309	8.9760	14.47598	20.186
8.8537	14.35374	20.226	8.9772	14.47719	20.162
8.8549	14.35494	20.210	8.9784	14.47839	20.189
8.8562	14.35617	20.140	8.9796	14.47959	20.216
8.8574	14.35737	20.270	8.9808	14.48080	20.102
8.8586	14.35860	20.216	8.9820	14.48200	20.170
8.8598	14.35980	20.191	8.9832	14.48321	20.126
8.8610	14.36101	20.181	8.9845	14.48448	20.138
8.8622	14.36221	20.195	8.9857	14.48568	20.187
8.8647	14.36473	20.268	8.9869	14.48687	20.128
8.8659	14.36594	20.206	8.9881	14.48808	20.154
8.8671	14.36714	20.184	8.9893	14.48928	20.164
8.8683	14.36834	20.139	8.9905	14.49050	20.160
8.8696	14.36955	20.167	8.9917	14.49170	20.233
8.8708	14.37076	20.194	8.9929	14.49289	20.153
8.8720	14.37197	20.236	8.9941	14.49410	20.140
8.8732	14.37317	20.164	8.9953	14.49530	20.162
8.8744	14.37438	20.171	8.9965	14.49650	20.115
8.8756	14.37559	20.245	8.9977	14.49771	20.088
8.8768	14.37679	20.152	8.9989	14.49892	20.176
8.8780	14.37800	20.299	9.0001	14.50013	20.145
8.8792	14.37920	20.193	9.0013	14.50133	20.166
8.8804	14.38042	20.163	9.0025	14.50253	20.093
8.8816	14.38162	20.239	9.0078	14.50782	20.120
8.8828	14.38282	20.214	9.0090	14.50903	20.158
8.8840	14.38403	20.271	9.0102	14.51024	20.199
8.8852	14.38523	20.282	9.0115	14.51145	20.102
8.8864	14.38644	20.280	9.0127	14.51265	20.149
8.8877	14.38765	20.344	9.0138	14.51385	20.171
8.8888	14.38885	20.293	9.0151	14.51506	20.129
8.8901	14.39006	20.363	9.0163	14.51627	20.327
8.8913	14.39127	20.289	9.0175	14.51749	20.310
8.8925	14.39249	20.362	9.0206	14.52065	20.322
8.8939	14.43896	20.548	9.0218	14.52185	20.275
8.9402	14.44017	20.534	9.0231	14.52306	20.379
8.9414	14.44138	20.467	9.0243	14.52426	20.248
8.9426	14.44259	20.522	9.0255	14.52546	20.368
8.9438	14.44378	20.519	9.0267	14.52667	20.343
8.9450	14.44500	20.514	9.0279	14.52788	20.374
8.9462	14.44619	20.497	9.0291	14.52909	20.357
8.9474	14.44741	20.458	9.0303	14.53029	20.532
8.9486	14.44861	20.469	9.0315	14.53150	20.501
8.9498	14.44981	20.438	9.0327	14.53272	20.473
8.9510	14.45103	20.501	9.0339	14.53392	20.455
8.9522	14.45223	20.397	9.0351	14.53514	20.426
8.9534	14.45345	20.515	9.0363	14.53634	20.403
8.9547	14.45465	20.467	9.0375	14.53753	20.577
8.9559	14.45586	20.415	9.0387	14.53873	20.491
8.9571	14.45706	20.356	9.0399	14.53993	20.558

^a At beginning of exposure**Table 1.** *cont'd*

UT ^a	JD ^a	m _v	UT ^a	JD ^a	m _v
Feb. 02	2452300+		Feb. 02	2452300+	
9.0411	14.54113	20.450	9.8495	15.34946	20.559
9.0423	14.54235	20.485	9.8507	15.35067	20.555
9.0435	14.54355	20.536	9.8519	15.35187	20.628
9.0448	14.54477	20.582	9.8548	15.35485	20.600
9.0460	14.54597	20.636	9.8560	15.35605	20.545
9.0472	14.54718	20.500	9.8573	15.35726	20.587
9.0484	14.54839	20.465	9.8585	15.35846	20.583
9.0496	14.54961	20.553	9.8597	15.35966	20.526
9.0508	14.55081	20.629	9.8609	15.36087	20.561
9.0520	14.55201	20.567	9.8621	15.36206	20.626
9.0532	14.55323	20.593	9.8633	15.36326	20.443
9.0544	14.55444	20.502	9.8645	15.36447	20.590
9.0557	14.55566	20.577	9.8657	15.36567	20.587
9.0673	14.56730	20.569	9.8669	15.36689	20.611
9.0685	14.56852	20.584	9.8681	15.36809	20.567
9.0697	14.56973	20.570	9.8693	15.36929	20.502
9.0709	14.57094	20.546	9.8705	15.37049	20.545
9.0722	14.57215	20.510	9.8717	15.37169	20.515
9.0734	14.57336	20.448	9.8729	15.37289	20.495
9.0745	14.57455	20.438	9.8741	15.37410	20.531
9.0758	14.57575	20.492	9.8753	15.37530	20.483
9.0770	14.57696	20.363	9.8765	15.37650	20.554
9.0782	14.57816	20.476	9.8777	15.37771	20.413
9.0794	14.57939	20.552	9.8789	15.37891	20.482
9.0806	14.58059	20.433	9.8801	15.38012	20.373
9.0818	14.58179	20.472	9.8813	15.38132	20.468
9.0830	14.58300	20.510	9.8825	15.38252	20.406
9.0842	14.58420	20.378	9.8837	15.38373	20.428
9.0854	14.58539	20.519	9.8849	15.38493	20.453
9.0866	14.58661	20.496	9.8861	15.38613	20.416
9.0878	14.58781	20.507	9.8873	15.38734	20.297
9.0890	14.58903	20.520	9.8885	15.38853	20.331
9.0902	14.59024	20.505	9.8897	15.38975	20.279
9.0915	14.59147	20.535	9.8909	15.39095	20.333
9.0927	14.59269	20.365	9.8922	15.39215	20.354
9.0939	14.59389	20.304	9.8934	15.39336	20.364
9.0951	14.59512	20.266	9.8946	15.39456	20.274
9.0963	14.59631	20.350	9.8958	15.39575	20.329
9.0976	14.59755	20.278	9.8970	15.39696	20.455
9.0987	14.59875	20.336	9.8982	15.39816	20.324
9.0999	14.59995	20.260	9.8994	15.39936	20.286
9.1012	14.60115	20.338	9.9006	15.40057	20.200
9.1024	14.60235	20.310	9.9018	15.40177	20.293
9.8284	15.32839	20.649	9.9034	15.40337	20.287
9.8296	15.32961	20.543	9.9046	15.40458	20.223
9.8308	15.33081	20.632	9.9058	15.40578	20.207
9.8320	15.33201	20.567	9.9070	15.40699	20.210
9.8332	15.33322	20.486	9.9082	15.40818	20.158
9.8344	15.33442	20.649	9.9094	15.40939	20.096
9.8356	15.33563	20.654	9.9106	15.41058	20.233
9.8368	15.33684	20.468	9.9118	15.41178	20.261
9.8380	15.33803	20.532	9.9130	15.41300	20.130
9.8393	15.33926	20.502	9.9142	15.41420	20.254
9.8405	15.34047	20.630	9.9154	15.41541	20.119
9.8417	15.34170	20.492	9.9166	15.41661	20.235
9.8435	15.34345	20.600	9.9178	15.41780	20.179
9.8447	15.34465	20.675	9.9190	15.41900	20.171
9.8459	15.34586	20.612	9.9202	15.42021	20.159
9.8471	15.34706	20.567	9.9214	15.42141	20.117
9.8483	15.34825	20.561	9.9226	15.42262	20.171

^a At beginning of exposure

Table 1. *cont'd*

UT ^a	JD ^a	m _v	UT ^a	JD ^a	m _v
Feb. 02	2452300+		Feb. 02	2452300+	
9.9238	15.42381	20.201	10.0172	15.51723	20.261
9.9250	15.42501	20.233	10.0184	15.51845	20.352
9.9262	15.42623	20.159	10.0197	15.51965	20.437
9.9274	15.42743	20.248	10.0209	15.52086	20.417
9.9287	15.42865	20.274	10.0221	15.52207	20.356
9.9298	15.42985	20.229	10.0233	15.52326	20.370
9.9311	15.43105	20.197	10.0245	15.52447	20.265
9.9323	15.43226	20.211	10.0257	15.52567	20.258
9.9335	15.43346	20.248	10.0269	15.52687	20.229
9.9347	15.43466	20.240	10.0281	15.52808	20.371
9.9359	15.43587	20.213	10.0293	15.52927	20.339
9.9371	15.43706	20.311	10.0305	15.53047	20.207
9.9383	15.43826	20.287	10.0317	15.53169	20.287
9.9395	15.43947	20.252	10.0329	15.53289	20.118
9.9407	15.44066	20.213	10.0341	15.53410	20.261
9.9418	15.44185	20.208	10.0353	15.53531	20.131
9.9431	15.44306	20.211	10.0365	15.53652	20.193
9.9443	15.44426	20.300	10.0377	15.53771	20.076
9.9454	15.44545	20.307	10.0389	15.53891	20.108
9.9467	15.44666	20.238	10.0401	15.54013	20.152
9.9479	15.44787	20.400	10.0413	15.54133	20.195
9.9491	15.44907	20.336	10.0426	15.54255	20.212
9.9503	15.45028	20.323	10.0437	15.54374	20.087
9.9520	15.45205	20.402	10.0473	15.54734	20.083
9.9533	15.45325	20.393	10.0485	15.54854	20.200
9.9545	15.45446	20.434	10.0498	15.54975	20.196
9.9557	15.45566	20.408	10.0510	15.55096	20.176
9.9569	15.45686	20.362	10.0522	15.55216	20.166
9.9581	15.45807	20.355	10.0534	15.55337	20.193
9.9593	15.45928	20.416	10.0569	15.55688	20.247
9.9605	15.46047	20.528	10.0581	15.55809	20.138
9.9617	15.46169	20.522	10.0593	15.55929	20.113
9.9629	15.46291	20.467	10.0605	15.56049	20.235
9.9641	15.46411	20.458	10.0617	15.56169	20.157
9.9653	15.46530	20.569	10.0629	15.56289	20.180
9.9665	15.46650	20.475	10.0641	15.56409	20.250
9.9677	15.46770	20.612	10.0653	15.56530	20.275
9.9689	15.46891	20.586	10.0665	15.56650	20.220
9.9961	15.49612	20.411	10.0677	15.56771	20.293
9.9973	15.49733	20.487	10.0689	15.56891	20.185
9.9985	15.49854	20.432	10.0701	15.57012	20.343
9.9998	15.49976	20.522	10.0713	15.57132	20.180
10.0009	15.50095	20.618	10.0725	15.57251	20.317
10.0088	15.50881	20.402	10.0737	15.57372	20.097
10.0100	15.51001	20.467	10.0749	15.57492	20.346
10.0112	15.51122	20.400	10.0761	15.57612	20.285
10.0124	15.51243	20.371	10.0773	15.57734	20.273
10.0136	15.51363	20.330	10.0785	15.57854	20.262
10.0148	15.51483	20.396	10.0797	15.57975	20.264
10.0160	15.51604	20.382	10.0809	15.58095	20.326

^a At beginning of exposure

certainty resulting from a sinusoidal fit of the 341 data points. Figure 1 shows the data as a function of time, and then phased to the 3.1757 h period. A reference 0.25 phase is taken on Julian date 2452314.3591, corresponding to a brightness maximum. Plotting the data phased to a double period (6.3514 hr) suggests an asymmetry between the two maxima, in agreement with JS02. However, given the

± 0.06 magnitude uncertainty in our data, we more conservatively retain the single-peaked period, for which, from an error estimate based on Horne & Baliunas (1986), we adopt a 3.176 ± 0.010 h value. JS02 obtained a much more accurate 3.1721 ± 0.0001 hr single-peaked period. We note however that with such a period, our Feb. 2002 observations appear out of phase from their Feb. 2001 observations by $\sim 95 \pm 30^\circ$. JS02 note that periods of 3.1656 hr and 3.1788 hr are alternate acceptable fits to their data. While the first one would produce again a $\sim 99^\circ$ mismatch with our data, the second one would give a much better agreement ($\sim 18^\circ$ phase difference, i.e. 10 minutes, which is reduced to zero assuming a 0.0001 hr uncertainty on the period). We also note that with a period of 6.3576 hr ($= 2 \times 3.1788$ hr), the lightcurve asymmetry we tentatively observe would be in phase with the one reported by JS02 (i.e. a primary maximum in their curve is in phase with a primary maximum in ours). To phase the thermal observations below, we will finally adopt $P = 3.1788$ hr.

2.2. Thermal observations

Thermal observations were conducted with the IRAM 30-m radiotelescope on five dates in January - February 2002. We used the Max Planck Institut für Radio Astronomie 37 element bolometer array (Kreysa et al. 1998). The beams have a half-power width of 11" and are separated by $\sim 20''$. The instrument has a bandwidth of about 60 GHz, and an effective frequency close to 250 GHz (1.2 mm). Observations of Varuna were performed in "on-off" mode, in which the subreflector (or wobbler) of the telescope was alternately (with a 2 Hz frequency) looking at the target and at a sky position 32" away in azimuth (either to the left or right of the source, alternating every 10 s). While this procedure subtracts most of the atmospheric emission, the photometric accuracy is determined in part by the ability to eliminate its temporal fluctuations. Our multibeam observations allow us to estimate the latter from the channels adjacent to the central channel.

Observations were conducted as follows. Pointing and focus of the telescope were first determined by measurements on Callisto. Then, the zenithal atmospheric opacity was measured from sky measurements at several elevations (skydip). Then, on-off measurements were performed during about 40-50 minutes (9-11 loops of 20 10-sec subscans, plus overheads). This entire procedure provided one "Varuna measurement". Three such measurements were obtained on January 19, in visitor mode. Several additional measurements were obtained subsequently as "pooled observations" (i.e., service mode): two on January 28, and one on January 31, February 11 and February 12. Observations were performed in good weather conditions (1-2 mm water). Most importantly, atmospheric stability was good, except on February 11 and 12, where large fluctuations of the zenithal sky opacity occurred. In addition, data reduction revealed that one of the two measurements

Table 2. IRAM 30-m observations

Date	UT ^a	Phase ^b	τ ^c	F_{adj}^d (mJy)	F^e (mJy)
2002/01/19 01h15	0.157	0.18	1.7	1.4 ± 1.0	
2002/01/19 02h23	0.513	0.18	0.8	3.3 ± 1.0	
2002/01/19 03h30	0.864	0.18	0.2	1.5 ± 1.0	
2002/01/28 20h59	0.315	0.17	1.2	0.8 ± 1.0	
2002/01/31 22h30	0.442	0.14	-0.2	-0.1 ± 0.7	

^a UT time at the middle of integration

^b See text for phase reference. Phases of 0.25 and 0.75 (resp. 0 and 0.5) correspond to maxima (resp. minima) of the visible lightcurve.

^c Mean zenithal atmospheric opacity

^d Mean flux in the six channels adjacent to central channel

^e Varuna flux, after subtraction of F_{adj} from central channel

of Jan. 28 suffered from a large focus error. Thus, these three measurements were not considered, leaving us with a total of five individual measurements of Varuna’s 1.2 mm flux.

For each measurement, the data were reduced in terms of a “count number” for each channel. Relative calibration of the 37 channels were achieved by using a 180” x 140” on-the-fly map (Wild 1999) obtained on Mars on January 25, 2002. Absolute calibration was obtained from Mars on-off measurements on each observing day. Table 2 summarizes the five Varuna measurements and Fig. 2 illustrates the detection of the object in the grand total data average. For each measurement, Table 2 gives the mean flux level in the innermost ring of 6 channels (see Fig. 2); this value was subtracted from the central channel to yield Varuna’s flux. We believe that the flux variability at the mJy level seen in Table 2 is primarily due to atmospheric fluctuations, rather than to background sources. To contribute at a 0.1 mJy level, a 4000 K star would have to be brighter than $V \sim 7.5$. Background galaxies may be a more important issue. The density of faint background galaxies brighter than 1 mJy at 250 GHz (2 mJy at 350 GHz) is 3000/dg² according to the most recent JCMT/SCUBA survey (Borys et al. 2002). The probability that such a source falls within the central channel is only 0.02, however the probability that one of the six adjacent channels is affected at the mJy level is 10-15 %. This might contribute to the fact that the mean flux over these channels is generally positive. However, if this were dominantly the case, this “mean background flux” should not vary, as it seems to do, over a 1-hour timescale (during which the source moves by only 3”). We thus believe that the residual flux mostly reflects sky fluctuations, justifying our approach to subtract it from the central channel. Using only the inner 6 channels to estimate and remove this contribution is justified by the fact that using more channels would increase the probability of including an unidentified background source. In addition, we believe that using only the closest adjacent channels is the most adequate way to evaluate the sky contribution in the central channel. Correction of the cosmic background is entirely negligible (0.004 mJy).

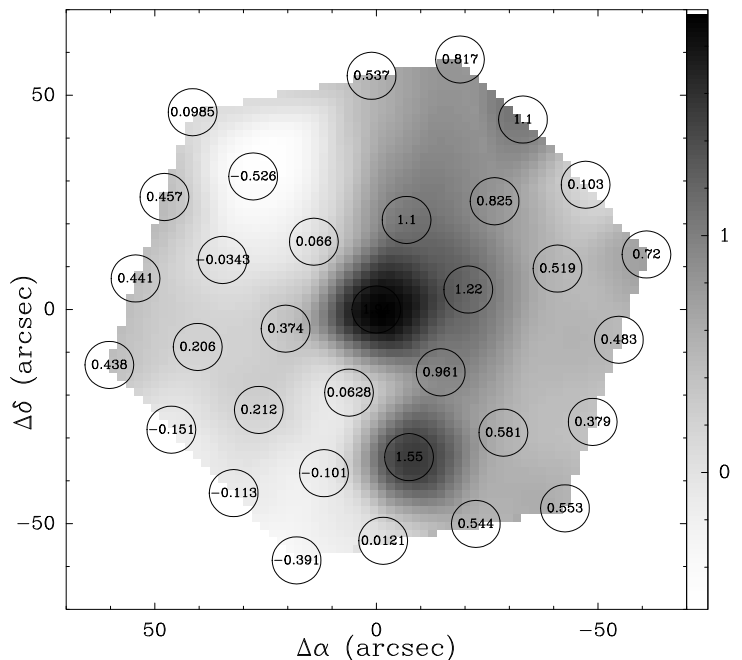


Fig. 2. The detection of Varuna in the IRAM 37-element bolometer array. This image corresponds to the grand average of all data. Numbers indicate the flux levels (mJy) in each of the bolometers (except in four bad channels). The central channel is at 1.97 mJy.

3. Interpretation

In Fig. 3, the five thermal flux measurements are plotted as a function of phase, assuming a period of 3.1788 hr and the same reference phase. The data are much too noisy to search for any possible correlation with the visible lightcurve (and hence to discriminate between a shape vs. albedo origin for the latter). Averaging all Varuna measurements leads to a flux of 1.12 ± 0.41 mJy. This is only a 2.7 σ detection; together with the 3.3 σ detection of JAE01, this illustrates the difficulty of such measurements.

This measurement is analyzed using a thermal model, developed for Pluto (Lellouch et al. 2000a, 2000b), and following a classical formulation (Spencer et al. 1989). The local temperature is written as:

$$T = \left[\frac{1 - A_b}{\epsilon_b} \frac{F}{\sigma R^2} \right]^{1/4} f(\text{latitude}, \text{local time}, \Theta)$$

where A_b is the bolometric albedo and ϵ_b is the bolometric emissivity. $F/(\sigma R^2) = 60.0$ K is the instantaneous equilibrium temperature at Varuna’s current heliocentric distance ($R = 43.105$ AU) and at the subsolar point for $\epsilon_b = 1$, $A_b = 0$. f symbolically represents the normalized temperature function, as a function of *latitude*, *local time* and of the thermal parameter Θ . At a given wavelength (λ), the local flux is then equal to $\epsilon_\lambda B_\lambda(T/\eta)$, where ϵ_λ is the spectral emissivity, and η is a factor accounting for the beaming effect. The local fluxes are then weighted by the solid angles sustained and added. At the low precision of our measurements, a number of assumptions can be

safely made. First, A_b can be considered as known. Based on JAE01’s estimate of Varuna’s red geometric albedo (p_r) and color, and the observed correlation between p_v and the phase integral q (Lellouch et al. 2000a), we assume $q = 0.4$. The resulting bolometric albedo is $A_b \sim 0.02$ - 0.03 . With the $(1-A_b)^{0.25}$ dependence of the equilibrium temperature, the thermal flux is essentially insensitive to p_v . Second, with a rotation period of 3.17 hr, Varuna is likely to be in the “fast rotator” regime: assuming a thermal inertia similar to Pluto’s ($\Gamma \sim 3 \times 10^4$ erg cm $^{-2}$ s $^{-1/2}$ K $^{-1}$ Lellouch et al. 2000a), the resulting thermal parameter is $\Theta \sim 600$ (as opposed to 3–20 for Pluto), so that diurnal temperature variations should be negligible. Although Varuna’s pole orientation is unknown, the large amplitude of the lightcurve suggests that the subearth and subsolar points are closer to the equatorial plane than to the polar axis. We thus adopt an isothermal latitude model with the Sun in the equatorial plane. Based on an analogy with Pluto (Lellouch et al. 2000a), we assume a bolometric emissivity of 0.9. With these assumptions, the local temperature is simply $T = T_{eq} \times \cos^{0.25}(\text{latitude})$, where the equatorial temperature is $T_{eq} = 45.9$ K. Again by similarity with Pluto (Lellouch et al. 2000b), we assume a millimeter-wave emissivity of 0.7. For simplicity, we neglect any beaming effect, i.e. set $\eta = 1$. We then integrate the thermal flux over the object’s disk and solve the mean measured flux for its mean equivalent circular diameter. We find $D = 1060_{-220}^{+180}$ km. Although our central flux value, when rescaled to 850 μm , is 25–30 % lower than JAE01’s, our inferred nominal value is slightly higher than theirs; this is due to different assumptions on the millimeter emissivity, the distribution of temperature, and the fact that JAE01 adopted the Rayleigh-Jeans approximation (which is relatively inaccurate at 0.8 mm – about 20 % error for $T = 45$ K). With our model, we would infer a 1220_{-200}^{+175} km diameter from JAE01’s measurements. The two determinations nonetheless overlap within error bars. The above estimates assume that Varuna is a single object and that its lightcurve is due either to albedo spots or a non-spherical shape. If Varuna is a binary (although, as noted by JS02, its quasi-sinusoidal lightcurve tends to argue against it), our measurements would indicate diameters of ~ 950 and ~ 660 km for the two components.

The associated (i.e., averaged over the rotation of the object) V magnitude is $m_v = 20.37 \pm 0.08$. With a mean V - R = 0.64 (JS02), this gives $m_r = 19.73$, in agreement with earlier measurements. The rotationally-averaged geometric albedo (p) in a given color is then computed from the usual equation:

$$p\phi = 4\left(\frac{R\Delta}{D}\right)^2 10^{0.4(m_{sun} - m_{obj})}$$

where R is the heliocentric distance in AU, Δ and D are the geometric distance and object’s diameter in the same units, m_{sun} and m_{obj} are the magnitude of the Sun and Varuna in the same color ($m_{sun} = -26.74$ in V and -27.1 in R), and ϕ is the phase function at the relevant phase angle. We neglect any phase angle effects, i.e. set $\phi = 1$. With

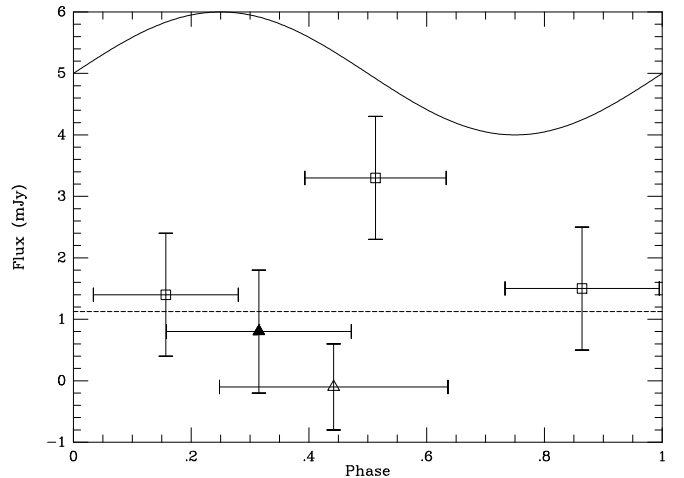


Fig. 3. Thermal measurements of Varuna, obtained on Jan. 19 (open squares), Jan. 28 (filled triangle) and Jan. 31 (open triangle), plotted as a function of phase. A 3.1788 hr period and a 0.25 phase on Julian date 2452314.3591 are used. The horizontal “error bars” indicates the range of phase sampled by the individual measurements. The dashed line indicates the average flux level. The solid line schematically represents the variation of the visible flux with phase.

the above diameter and the mean conditions for the visible observations ($\Delta = 42.35$ AU, $R = 43.105$ AU), we obtain a mean $p_v = 0.038_{-0.010}^{+0.022}$ and $p_r = 0.049_{-0.013}^{+0.029}$. Although nominally smaller, this again is consistent within error bars with the JAE01 determinations. Note that the 30–40 % uncertainty in the albedo determination is dominated by the uncertainty in the diameter (i.e. in the thermal flux), the 0.08 mag absolute photometric uncertainty having a much smaller effect (8 % error).

4. Summary

We have performed coordinated optical and thermal observations of Trans-Neptunian object (20000)Varuna. The optical data, acquired at the IAA 1.5 m telescope, show a clear lightcurve with a single-peaked period of 3.176 ± 0.010 hr, a mean V magnitude of 20.37 ± 0.08 and a 0.42 ± 0.01 magnitude amplitude. Phasing our observations with those of Jewitt & Sheppard (2002), we find a best fit period of 3.1788 ± 0.0001 hr. Our observations tentatively confirm an asymmetry in the lightcurve, as first reported by Jewitt & Sheppard. This would favor the hypothesis that the lightcurve is actually double-peaked with a 6.3576 ± 0.0002 hr period and predominantly due to an elongated shape of the object. The thermal data, obtained with the IRAM 30-m telescope, consist of five independent measurements of Varuna’s 1.2 mm flux, sampling the optical lightcurve. These measurements are much too noisy to distinguish a possible thermal lightcurve. Averaged together, they indicate a 1.12 ± 0.41 mJy flux at 1.2 mm, i.e. a 2.7σ detection that adds to the 3.3σ detection of Jewitt, Aussel & Evans (2001)

at 0.8 mm and confirms the difficulty of this kind of observations. Assuming emissivity and thermophysical surface properties similar to Pluto's, the thermal data indicate a mean equivalent circular diameter of 1060_{-220}^{+180} km. The associated albedos in the visible and the red are $p_v = 0.038_{-0.010}^{+0.022}$ and $p_r = 0.049_{-0.013}^{+0.029}$, respectively, consistent with the determination by JAE01. Taken together with the albedo measurement of 1993 SC ($p_v = 0.022_{-0.006}^{+0.013}$) and the possible detection of 1996 TL₆₆ by Thomas et al. (2000), this indicates that the canonical 0.04 albedo adopted for size distribution studies is not invalid at this point.

Acknowledgments: This research is partially based on data taken at the 1.5m telescope of Sierra Nevada Observatory which is operated by the Consejo Superior de Investigaciones Científicas through the Instituto de Astrofísica de Andalucía. N.P. acknowledges funding from the FCT, Portugal (ref: SFRH/BD/1094/2000).

References

- Altenhoff, W.J., J.W.M. Baars, J.B. Schraml, et al. 1996, A & A 309, 953
- Barucci, M. A., Romon J., Doressoundiram A., & Tholen D. J. 2000, Astron. J. 120, 496
- Borys, C., S.C. Chapman, M. Halpern, & D. Scott 2002, MNRAS 330, L63
- Doressoundiram, A., M.-A. Barucci, J. Romon, & C. Veillet 2001, Icarus, 154, 277
- Doressoundiram, A., N. Peixinho, C. de Bergh, et al. 2002, ApJ, submitted.
- Duncan, M., J. Quinn, & S. Tremaine 1988, Ap. J. 328, L69
- Farnham, T.L. 2001, IAU Circ. 7583
- Horne, J.H., & S.L. Baliunas 1986, Ap. J. 302, 757
- Jewitt, D., & J. Luu 1992, in *Protostars and Planets IV*, (Univ. Arizona Press, Tucson), 1201.
- Jewitt, D., H. Aussel, & A. Evans 2001, Nature 411, 446
- Jewitt, D., & S.S. Sheppard 2002, A.J. 123, 2110.
- Knoffel, A. & R. Stoss 2000, MPEC. No 2000-Y45
- Kreysa, E., H.-P. Gemuend, J. Gromke et al. 1998, SPIE 3357, 319
- Landolt, A. U. 1992, Astron. J. 104, 340
- Lellouch, E., R. Laureijs, B. Schmitt, et al. 2000a, Icarus 147, 220
- Lellouch, E., G. Paubert, R. Moreno, & B. Schmitt 2000b, Icarus 147, 580
- Licandro, J., E. Oliva, & M. Di Martino 2001, A&A 373, L29.
- Lomb, N. R. 1976, Astroph. Space Sci. 39, 447
- McMillan, R.S., & J.A. Larsen 2000, MPEC. No 2000-X02
- Redman, R.O., P.A. Feldman, H.E. Matthews et al. 1992, A.J., 104, 405
- Spencer, J. R., A. L. Lebofsky & M. V. Sykes 1989. Icarus, 78, 337.
- Thomas, N., S. Eggers, W.-H. Ip et al. 2000, ApJ 534, 446
- Wild, W. 1999, www.iram.es/IRAMES/index.htm